Variation in key leaf photosynthetic traits across wheat wild relatives is accession dependent not species dependent

Lorna McAusland[1], Silvere Vialet-Chabrand[2], Iván Jauregui[3], Amanda Burridge[4], Stella Hubbart-Edwards[1], Michael J. Fryer[2], Ian P. King[1], Julie King[1], Kevin Pyke[1], Keith J. Edwards[4], Elizabete Carmo-Silva[3], Tracy Lawson[2] and Erik H. Murchie[1]

[1]Division of Plant and Crop Sciences, School of Biosciences, University of Nottingham, Sutton Bonington, Nottingham, LE12 5RD, UK; [2]School of Life Science, University of Essex, Wivenhoe Park, Colchester, CO4 3SQ, UK; [3]Lancaster Environment Centre, Lancaster University, Lancaster, LA1 4YQ, UK; [4]Life Sciences, University of Bristol, Bristol, BS8 1QU, UK

Author for correspondence:
Erik H. Murchie
Tel: +44 115 9516234
Email: erik.murchie@nottingham.ac.uk

Received: *4 May 2020*
Accepted: *3 July 2020*

New Phytologist (2020)
doi: 10.1111/nph.16832

Key words: genotyping, photosynthesis, Rubisco, stomata, *T. aestivum*, wild relatives.

Summary

- The wild relatives of modern wheat represent an underutilized source of genetic and phenotypic diversity and are of interest in breeding owing to their wide adaptation to diverse environments. Leaf photosynthetic traits underpin the rate of production of biomass and yield and have not been systematically explored in the wheat relatives.
- This paper identifies and quantifies the phenotypic variation in photosynthetic, stomatal, and morphological traits in up to 88 wheat wild relative accessions across five genera. Both steady-state measurements and dynamic responses to step changes in light intensity are assessed.
- A 2.3-fold variation for flag leaf light and CO_2-saturated rates of photosynthesis A_{max} was observed. Many accessions showing higher and more variable A_{max}, maximum rates of carboxylation, electron transport, and Rubisco activity when compared with modern genotypes. Variation in dynamic traits was also significant; with distinct genus-specific trends in rates of induction of nonphotochemical quenching and rate of stomatal opening.
- We conclude that utilization of wild relatives for improvement of photosynthesis is supported by the existence of a high degree of natural variation in key traits and should consider not only genus-level properties but variation between individual accessions.

Introduction

Modern hexaploid bread wheat cultivars are the product of a genetic bottleneck – a reduction in genetic diversity brought about by domestication through polyploidization and the intensive selection for agronomically important traits over the past 10 000 yr (Charmet, 2011; Faris, 2014). However, despite breeding efforts in recent years, increases in global yields have slowed – averaging between 0 and 1.1% annually (Dixon *et al.*, 2009). Potential yield gains have been circumvented by increasingly unpredictable environmental conditions, susceptibility to biotic stresses, and agronomic practices (Brisson *et al.*, 2010). During the processes of domestication and selection, modern wheat may have lost key alleles required for adaptive robustness to abiotic and biotic stress – a negative side effect resulting from single trait selection. With pressure to raise yields between 1.6 and 2.4% per annum over the next 50 yr (Brisson *et al.*, 2010; Ray *et al.*, 2013), the emphasis falls to increasing the genetic diversity of modern wheat to maintain or improve yields under current environmental conditions (Evans & Lawson, 2020).

The wild, uncultivated relatives of modern wheat provide a global and mostly underutilized source of genetic and phenotypic diversity (King *et al.*, 2017), with over 80 000 wheat accessions documented (*Crop Wild Relative Diversity*, 2019). The wild relatives represent adaptation to diverse habitats and climates, suggesting the existence of genes that are unavailable in the existing elite wheat germplasm. Exploration of the wild relatives may uncover previously untapped potential for wider and enhanced characteristics to face changing environmental conditions and disease resistance, ultimately aiming to improve the productivity and resilience of future modern varieties.

Wide crossing or hybridization events can be used as a means to generate plants with introgressions – fragments of wild relative DNA inserted into the genome of modern wheat. This approach can be used to markedly improve wheat genetic diversity (Chen *et al.*, 2012; Molnár-Láng *et al.*, 2014). Successful introduction has been noted in numerous species, including, but not limited to, *Aegilops umbellulata* (Sears, 1955, 1972), *Secale cereale* (Sebesta & Wood, 1978), *Aegilops ventricosa* (Doussinault *et al.*, 1983; Burt & Nicholson, 2011), *Aegilops speltoides* (King *et al.*, 2018), *Triticum urartu* (Grewal *et al.*, 2018a), and *Thinopyrum bessarabicum* (King *et al.*, 1997; Grewal *et al.*, 2018b) (Supporting Information Table S1).

Despite the high probability of discovering novel traits and genes, the current number of species and accessions already investigated as potential candidates for crop improvement is relatively

few. Though the majority of studies have generated lines that are resistant to biotic or abiotic stresses, a smaller proportion have reported the transfer of more complex polygenic traits, including yield stability, yield gains (Villareal *et al.*, 1996), and increases in photosynthetic rates (Austin *et al.*, 1982). Photosynthesis is a complex polygenic trait that fundamentally underpins the rate of production of biomass, and ultimately of yield. The close relationship demonstrated between enhanced photosynthetic CO_2 assimilation, biomass, and yield under elevated, ambient CO_2 supports the assumption that enhancing the capacity of individual leaves to fix carbon (C) will support higher yields though increased biomass (Long *et al.*, 2006; Zhu *et al.*, 2008, 2010, 2018; Murchie *et al.*, 2009).

The relationship between photosynthesis and biomass accumulation is a ubiquitous and cumulative process involving numerous, interconnected processes. For example, at the canopy level, canopy architecture can drastically change both the amount of intercepted light and the efficiency with which it is converted into biomass and yield (Murchie *et al.*, 2018; Wu *et al.*, 2019). At the leaf level, under optimal environmental conditions, strong positive correlations are observed between stomatal conductance, carboxylation capacity, and the rate of leaf CO_2 uptake (Wong *et al.*, 1979). Under saturating light, the Rubisco carboxylation efficiency and capacity are vital (Carmo-Silva *et al.*, 2015). Under fluctuating environmental conditions, asynchronies arise between the changes in light intensity and the limitations imposed by the components of Rubisco, stomatal conductance (g_s), and photoprotection (Lawson & Blatt, 2014; Kromdijk *et al.*, 2016; McAusland *et al.*, 2016; Taylor & Long, 2017; Lawson & Vialet-Chabrand, 2019; Murchie & Ruban, 2019), leading to restricted CO_2 assimilation and lowered water-use efficiency. Identifying species-specific rapid responses of stomata, photoprotection, and Rubisco is crucial in maximizing CO_2 uptake and minimizing water loss in response to a fluctuating field environment (Faralli *et al.*, 2019b). In addition, the anatomy of the leaf also has a large impact on the diffusion pathway of CO_2 from traits such as stomatal density and distribution (Pearson *et al.*, 1995; Faralli *et al.*, 2019b), the size of the intracellular spaces (Lundgren *et al.*, 2019), and the distance between veins (Richards, 2000; Terashima *et al.*, 2010; Reynolds *et al.*, 2012; Burgess *et al.*, 2015; Driever *et al.*, 2017).

The convergence of these traits provides a plethora of targets to improve photosynthesis, but natural genetic variation that can be used for breeding is unclear, especially in wheat (Driever *et al.*, 2014; Salter *et al.*, 2019). In some cases the underlying genes are known, along with the mechanism likely to underlie the improvement, and these currently rely on genetic modification to achieve both the proof of concept and the putative improved variety (e.g. Kromdijk *et al*, 2016). Clearly, the ability to combine discrete improvements will offer the greatest possibilities for yield improvement, and recent work has highlighted the need to improve photosynthesis in dynamic environments and across different climatic conditions (Tanaka *et al.*, 2019; Wu *et al.*, 2019; Faralli *et al.*, 2019a,b).

As wild relatives are increasingly used to introduce genetic diversity into modern cultivars it is key to rapidly identify potential candidates with higher photosynthetic rates and efficiencies, to determine the basis for these improvements, and to link the physiological and/or anatomical traits with gene discovery. These steps are not linear, and one process may inform the discovery of another. One of the limiting factors has been the inability to rapidly genotype large numbers of lines, but this has recently been overcome (King *et al.*, 2017; Devi *et al.*, 2019; Grewal *et al.*, 2020). Another significant bottleneck has been the availability of sophisticated high-throughput photosynthesis phenotyping tools. Recent advances in phenotyping techniques and pipelines provide the means to investigate variation on a larger scale – from screening populations of thousands to assessing the mechanistic basis behind that variation (McAusland *et al.*, 2015, 2019; Murchie *et al.*, 2018; Silva-Perez *et al.*, 2018; Araus *et al.*, 2018).

Here, we undertake a large-scale analysis of static and dynamic photosynthesis traits across accessions of wheat wild relatives. Our overall aim was to represent wide background adaptations, therefore we sourced these from a range of climates and continents across South America, western and eastern Europe, the Middle East, South and East Asia (Fig. 1). This work highlights for the first time the phenotypic and genomic diversity in the wild relatives as a source of variation for improving photosynthesis in modern wheat.

We show substantial variation in key traits, with specific wild accessions demonstrating a greater diversity and superior leaf photosynthesis in comparison with cultivated elite lines in both steady-state measurements and dynamic traits. These discoveries are important for developing strategies for selective inclusion into pre-breeding and breeding programmes.

Materials and Methods

Seed was obtained from the collection held by The Nottingham BBSRC Wheat Research Centre (University of Nottingham, Sutton Bonington, UK). A total of 88 accessions were investigated for variation in CO_2 and light-saturated photosynthesis, consisting of 41 species and five genera. A table of all plant material measured is presented in Table S2. Not all measurements were possible on all genotypes owing to the large variation in rates of growth and development. Accessions used were genotyped as a record that will be of use in future work to ensure that the same genotype was used across different/similar studies; these data are available at https://www.cerealsdb.uk.net/cerealgenomics/CerealsDB/indexNEW.php. All sample sizes n stated in this paper are the number biological replicates.

Assimilation rate–intercellular CO_2 analysis

Plants were grown and analysed at Sutton Bonington Campus, University of Nottingham. The wild relative accessions were germinated in compost (Levington M3; Everris, Ipswich, UK) and received 8 wk of vernalization at 5°C and a 16 h : 8 h, day : night cycle. The three modern *Triticum* cultivars received 4 wk of vernalization. After vernalization, all plants were moved to a glasshouse, potted into soil (John Innes No. 2; J. Arthur Bowers, Westland, Huntington, UK) and drip irrigated twice per day for 1 min with Hoagland's solution. The wild relatives were grown and measured between September 2016 and August 2018. Owing to differences in the rate of development of the wild

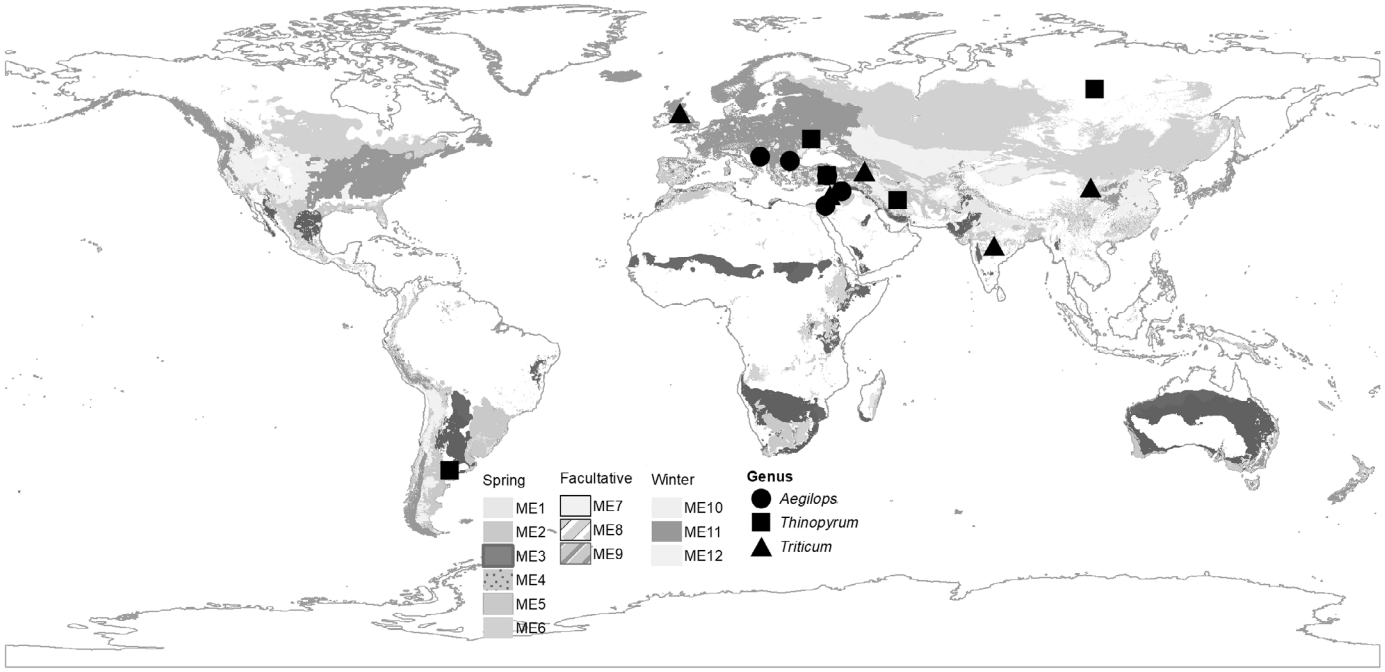

Fig. 1 A selection of the global origins of the wild relatives presented in this paper with genus indicated by shape: *Aegilops* (circles), *Triticum* (triangles), *Thinopyrum* (squares). The shading represents the 12 wheat mega-environments, typified by CIMMYT as broad, diverse growing environments, allowing targeted development of germplasm for improved yields globally (Rajaram *et al*., 1995).

relatives, the modern cultivars were grown and measured three times during this time period; September 2016–October 2016, November 2017–January 2018, and July–August 2018. The glasshouse was located at Sutton Bonington Campus, University of Nottingham, Leicestershire, UK (52°49′41.52″N, 1°14′54.60″W). Glasshouse conditions were maintained at 25 ± 2°C : 18 ± 2°C, day : night, under regular mildew, aphid, and thrip control measures applied following the manufacturer's recommendations. Photosynthetic photon flux density (PPFD) was maintained to achieve 16 h of light using supplemental lighting (HPS PL90E+ with Son-T Argo; Philips, Guildford, UK), applying up to 250 μmol m^{-2} s^{-1} PPFD at plant height when ambient PPFD fell below 500 μmol m^{-2} s^{-1}.

Using the flag leaf (Zadoks growth stage 4.1–4.5; Zadoks *et al*., 1974), the response of photosynthetic CO_2 assimilation rate A to 11 different external CO_2 concentrations C_a was measured. Leaf intercellular [CO_2] C_i and A were measured using an infrared gas analyser (LI-6400-XT; Li-Cor, Lincoln, NE, USA). Measurements started at an ambient C_a of 400 μmol mol^{-1} before C_a was decreased stepwise to a lowest concentration of 50 μmol mol^{-1}, then increased stepwise to an upper concentration of 1500 μmol mol^{-1}. Readings were recorded when A had stabilized to the new C_a (*c*. 2 min). To induce rapid responses, the leaf was exposed to a high saturating irradiance of 2000 μmol m^{-2} s^{-1}, using a 2 cm^2 leaf chamber with a blue–red LED light source. Leaf temperature and vapour pressure deficit were maintained at 25°C and 1.2 kPa, respectively.

The A–C_i response curves were fitted using the Farquhar *et al*. (1980) model using the R PLANTECOPHYS package (Duursma, 2015). The maximum velocity of Rubisco for carboxylation $V_{c,max}$ and the maximum rate of electron transport demand for ribulose 1,5-biphosphate (RuBP) regeneration J_{max} were estimated. All calculations were done in the R environment, v.3.5.0 (R Core Team, 2016).

Chl fluorescence imaging

Chl fluorescence imaging was performed on a subset of 25 wild relatives that represented good diversity in A–C_i responses and on three modern genotypes using a customized FluorCam imaging pulse-amplitude modulated fluorometer (Photon Systems Instruments, Brno, Czech Republic), as in McAusland *et al*. (2019). The same individual plants were used as those for the A–C_i analysis. Shutter time and sensitivity of the charge-coupled device were adjusted in accordance with the sample. The FluorCam was located in a temperature-controlled dark room maintained at 20 ± 2°C. Flag leaves were excised at 09:00 h and allowed to dark-adapt for 1 h in a custom imaging chamber. Fifteen minutes before the initial saturating pulse to determine F_v/F_m was taken, a pre-mixed gas of 400 μmol mol^{-1} CO_2 and 2% oxygen (O_2) was used to saturate the chamber to ensure consistent CO_2 and O_2 concentrations around the samples. The protocol consisted of three consecutive light steps of 15 min: 500, 100, and 1000 μmol m^{-2} s^{-1} PPFD (the latter is the capacity for the device). Saturating pulses were taken every minute throughout the protocol. The values of F_v/F_m and the responses of F_v'/F_m' (maximum efficiency of photosystem II (PSII) in the light), F_q'/F_m' (operating efficiency of PSII in the light), photochemical quenching (qP), and nonphotochemical quenching (NPQ) were extracted from each protocol (for an in-depth description of these parameters see Maxwell & Johnson, 2000; Baker, 2008; Murchie & Lawson, 2013).

To determine the rate of NPQ relaxation (under 100 μmol m^{-2} s^{-1} PPFD) and induction (1000 μmol m^{-2} s^{-1} PPFD), data

were fitted using a three-factor exponential function (Eqn 1)using the curve-fitting toolbox in MATLAB (R2018a; The MathWorks Inc., Natick, MA, USA) :

$$y = ae(-bx) + c \quad \text{Eqn 1}$$

where a determines the initial value, b is a constant representing the rate of exponential decay or growth and c is a constant describing the vertical shift in NPQ from start to end of the step.

$$y = ae^{-bx} \quad \text{Eqn 2}$$

(a, initial value; b, a constant representing the rate of exponential decay or growth). To determine the time t taken to achieve either 50% of the maximum NPQ values I_{50} or 50% of the maximum NPQ values R_{50}, the equations were solved for b and the following calculations applied:

$$t = \frac{1}{b}$$

$$I_{50} \text{ or } R_{50} = t \log_e(2)$$

(t, time constant; b, obtained from the rearrangement of either Eqn 1 or Eqn 2).

Leaf properties

Flag leaf adaxial absorbance for the leaves used in the Chl fluorescence screen (25 wild relative accessions and three modern genotypes) was measured using an integrating sphere (Li1800-12; Li-Cor) and spectroradiometer (ASD HandHeld 2: Hand-held VNIR; Malvern Panalytical, Boulder, CO, USA). Multiple flag leaves from the same plant were aligned to cover the measurement window if a single flag leaf was < 2cm^2. Absorbance was calculated in MATLAB (R2018a). Specific leaf area (SLA, m^2 kg^{-1}) was estimated following the protocol of Cornelissen *et al.* (2003); in brief, after photographing and measuring the fresh weight of the flag leaf, the leaves were placed in an oven at 70°C for 72 h. The leaves were reweighed to determine dry weight and the area calculated to produce SLA (IMAGEJ; Rasband, 1997–2018). Ear number per plant was also measured within this subset of plants.

Rubisco total activity and *in vitro* maximum carboxylation activity

Rubisco total activity was determined in flag leaves of glasshouse-grown plants (Sutton Bonington, University of Nottingham) for three modern *Triticum* cultivars (*Triticum aestivum*) and 19 wild relatives, from the same individual plants grown for A–C_i analysis in 2018 between the phenological Zadoks stages 4.2–5.5 (Zadoks *et al.*, 1974). Leaf segments were snap-frozen in liquid nitrogen (N_2) and stored at −80°C. Rubisco was extracted as described by Carmo-Silva *et al.* (2017), and Rubisco total activity was measured by the incorporation of $^{14}CO_2$ into acid-stable products at 30°C (Parry *et al.*, 1997). The radioactivity was measured by liquid scintillation counting (Packard Tri-Carb; PerkinElmer, Waltham, MA, USA). Total soluble protein (TSP) was quantified by the Bradford assay (Bradford, 1976).

Rubisco was extracted from flag leaf tissue of three modern wheat cultivars and six wild relatives. The maximum *in vitro* carboxylation rate V_{cmax} of fully activated Rubisco was determined (Prins *et al.*, 2016), incorporating the modifications described by Orr *et al.* (2016). Rubisco was quantified by the ^{14}C-carboxyarabinitol bisphosphate binding method of Whitney *et al.* (1999).

Stomatal dynamics

Twenty-one accessions were grown in glasshouses at the University of Essex (Colchester, UK). Seedlings were vernalized as described earlier and potted into 650 cm^3 pots containing peat-based compost (Levington F2S). Solar radiation provided a PPFD of *c.* 500 μmol m^{-2} s^{-1}, supplemented by sodium vapour lamps (600 W; Hortilux Schréder, Monster, the Netherlands) to 300 μmol m^{-2} s^{-1} PPFD when external PPFD dropped below 1200 μmol m^{-2} s^{-1} over a 10 h period. Air temperature was maintained at 25 ± 3°C during the day and 18 ± 3°C at night. The rapidity of the stomatal and photosynthetic responses was studied on fully expanded fourth leaves (growth stage Z1.4). Leaves were enclosed in a gas-exchange chamber (LCpro-SD; ADC BioScientific Ltd, Hoddesdon, UK) and left to equilibrate under dark conditions (*c.* 30 min). Gas exchange was recorded every 1 min for 5 min under dark conditions, and light was set to 1200 μmol m^{-2} s^{-1} for another 1 h. Leaf temperature was set at 25°C, leaf vapour pressure deficit was maintained at *c.* 1.2 kPa, and [CO_2] was set at 400 ppm. In order to describe the temporal response of stomatal conductance to water vapour g_s to a single step-change in PPFD, an analytical model derived from the model by Vialet-Chabrand and co-workers (Vialet-Chabrand *et al.*, 2013; McAusland *et al.*, 2016) was used. In brief, this dynamic model predicts the temporal response of g_s to PPFD using an asymmetric sigmoid function parameterized by specific time constants to describe the opening response of stomata.

Statistical analyses

Statistical analyses were conducted in R (http://www.r-project.org/). A Shapiro–Wilk test was used to test for normality, and a Levene test of homogeneity was used to determine if samples had equal variance. Single factor differences were analysed using a one-way ANOVA with a Tukey–Kramer honest significant difference test where more than one group existed or using a Student's *t*-test where only two groups were compared. For analysing more than two dependent variables, a MANOVA was used.

Results

Diversity of photosynthetic responses

A–C_i response curves were used to determine a 2.3-fold difference in light and CO_2-saturated photosynthetic assimilation A_{max}

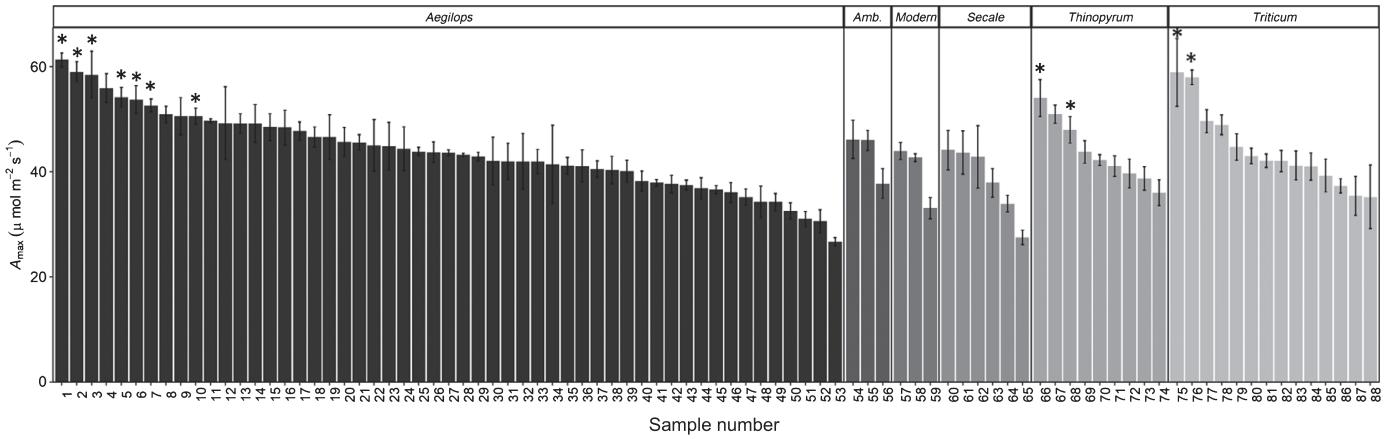

Fig. 2 CO_2 and light-saturated rates of photosynthetic assimilation A_{max} of modern *Triticum* varieties (modern) are compared against five wild relative genera: *Aegilops*, *Ambylopyrum* (*Amb.*), *Secale*, *Thinopyrum*, and *Triticum*. Measurements were made on fully developed flag leaves (decimal code: GS39) of glasshouse grown plants. Values are means and SE (n = 3–25). Asterisks indicate significantly different A_{max} values compared with one of the three modern *Triticum* varieties ($P < 0.05$).

between 88 accessions across five genera (Fig. 2). Overall, the modern varieties did not show a higher A_{max} than the wild relatives, and the variation was largely accession dependent, not species dependent. Of the 88 accessions, 11 wild relatives demonstrated significantly higher values of A_{max} ($P < 0.05$) than at least one of the three modern *Triticum* cultivars measured. Significant differences were observed between the individual accessions ($P < 0.0001$, $F_{(88,477)} = 5.71$) and genera ($P = 0.0016$, $F_{(5,560)} = 3.96$; see Fig. S1a). *Secale* A_{max} values were significantly lower than all other wild relative genera ($P < 0.03$), but not significantly different to the modern *Triticum*. It is notable that A_{max} for many accessions exceeded that seen in elite lines (38.4–47.0 μmol m^{-2} s^{-1}; Driever *et al.*, 2014).

Accession and genus-specific significant differences in maximum rate of carboxylation V_{cmax} ($P < 0.0001$) and electron transport J_{max} ($P < 0.0001$) were also observed (Fig. 3). Contrary to expectations, modern wheat did not have a higher J_{max} or V_{cmax} than many of the wild relatives. *Triticum dicoccoides* P95-98-3.2 (#75) demonstrated the highest V_{cmax} (240.6 ± 26.3 μmol m^{-2} s^{-1}) and J_{max} (313.5 ± 75.1 μmol m^{-2} s^{-1}), whereas the highest modern cultivar, *T. aestivum* 'Paragon' (#58), achieved 136.2 ± 25.5 μmol m^{-2} s^{-1} and 198.6 ± 24.5 μmol m^{-2} s^{-1}, respectively. Again it is notable that J_{max} and V_{cmax} seen here for many accessions exceeded that seen in previously reported elite lines (233–280 μmol m^{-2} s^{-1} and 124–161 μmol m^{-2} s^{-1}, respectively; Driever *et al.*, 2014).

The *Aegilops* genus exhibited the greatest variation in V_{cmax} and J_{max} (5.8 and 4.4-fold, respectively; Fig. S1b,c), whereas the values of the modern *Triticum* cultivar were more conserved (2.7 and 2.4-fold, respectively). *Secale* accessions had significantly lower V_{cmax} and J_{max} ($P < 0.05$) than the *Aegilops*, *Thinopyrum*, and wild and modern *Triticum* genera. Overall, the ratio $V_{cmax} : J_{max}$ (Fig. 3) was significantly ($P < 0.05$) lower in the modern *Triticum* cultivars than in *Secale*, *Thinopyrum*, *Amblyopyrum* and *Aegilops* genera, but not significantly different to the wild relative *Triticum* ($P = 0.23$).

$V_{cmax} : J_{max}$ has been suggested to indicate the limiting step of CO_2 assimilation, which is estimated by the transition point at which A shifts from being Rubisco to RuBP limited ($C_{itransition}$). $C_{itransition}$ was significantly different between accessions ($P < 0.0001$) and genera ($P < 0.0001$) (Fig. S2a). Ranging between 197.73 and 455.36 μmol mol^{-1} CO_2, the modern *Triticum* genus demonstrated the lowest $C_{itransition}$ values (258 ± 65.16 μmol mol^{-1}), whereas members of the *Secale* (307.38 ± 117.74 μmol mol^{-1}) were the highest (Fig. S2b).

The amount of TSP and Rubisco total activity (RV_t) were used to quantify the investment of 19 accessions into leaf rubisco (Fig. 4). The ratio of RV_t to TSP was broadly genus specific, with modern *Triticum* showing considerably higher RV_t for similar values of TSP. This higher RV_t is likely to represent a greater investment of modern *Triticum* in Rubisco protein, since *in vitro* V_{cmax} was not significantly different between genera (Fig. S3).

Genus and accession-specific differences were determined for TSP ($P < 0.02$) and RV_t ($P < 0.0001$), although the modern *Triticum* cultivars were only found to have significantly higher TSP ($P < 0.02$) compared with the *Amblyopyrum* accessions. These modern cultivars had significantly higher RV_t ($P < 0.003$) when compared with the five genera studied. Cultivar *T. aestivum* 'Paragon' exhibited 3.2-fold greater RV_t than *Aegilops muticum* 2130004 did, which had the lowest activity of the accessions studied (31.9 ± 9.0 μmol CO_2 m^{-2} s^{-1}).

Dynamic photosynthesis

The responses of 27 accessions in Chl fluorescence parameters to step changes in PPFD were analysed (Fig. S4; Table S3). This technique was utilized to uncover variation in dynamic photosynthetic traits; for example, in the speed of induction on transfer to high light or the kinetics of decay on transfer to low light (Fig. S4a). For a summary of the significant interactions for each light step, see Table S3. At steady state, the greatest number of significant differences were found under high light (1000 μmol m^{-2} s^{-1} PPFD). Maximum PSII efficiency in the light (F_v'/F_m') under 1000 μmol m^{-2} s^{-1} PPFD was significantly higher in the *Secale* than in the wild relative *Triticum*, *Aegilops* and *Amblyopyrum* genera ($P < 0.05$), whereas no significant

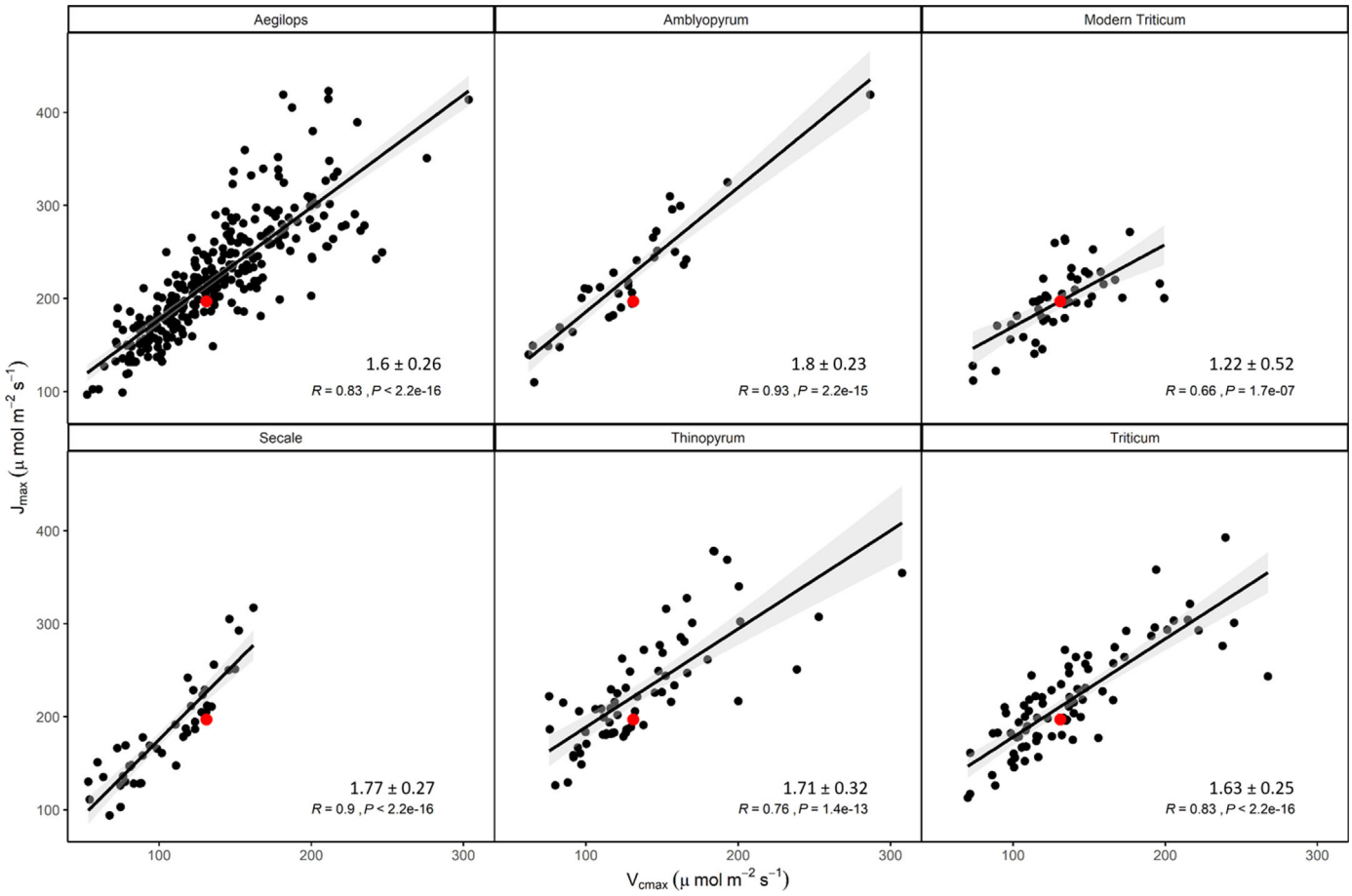

Fig. 3 The correlation between maximum rate of carboxylation V_{cmax} and electron transport J_{max} for 88 accessions across six genus groups. Data are individual points (n = 3–25 biological replicates). The average ratio J_{max} : V_{cmax} was calculated for each genus (micromoles of electrons per micromole of CO_2) ± SD (Carmo-Silva *et al*., 2017). A linear regression was fitted to all data within each genus and a Pearson's correlation coefficient calculated. The mean V_{cmax} and J_{max} for the modern *Triticum* genus is indicated on each plot by a red circle.

differences were determined between the genera under 500 or 100 μmol m^{-2} s^{-1} PPFD. Similarly, no significant differences were determined under any light intensity between the modern *Triticum* cultivars and the five wild relative genera.

In general, accessions from the *Amblyopyrum* and *Aegilops* genera achieved the highest values of PSII operating efficiency (F_q'/F_m'; Fig. S4b) and electron transport rate (ETR) under 500 and 1000 μmol m^{-2} s^{-1} PPFD. These values were consistently, significantly higher ($P < 0.05$) than in the accessions from the wild and modern *Triticum* genera. Under low light (100 μmol m^{-2} s^{-1} PPFD), the *Secale* genus achieved significantly ($P < 0.05$) higher F_q'/F_m' and ETR than the wild *Triticum* accessions did. By contrast, the wild and modern *Triticum* accessions achieved significantly higher values of NPQ under 500 and 1000 μmol m^{-2} s^{-1} PPFD intensities than the *Secale* and *Amblyopyrum* accessions did. The wild and modern *Triticum* also maintained the highest NPQ at 100 μmol m^{-2} s^{-1} PPFD when compared with *Secale* and *Amblyopyrum*. It was notable that those genera achieving the highest values of NPQ under 1000 μmol m^{-2} s^{-1} PPFD also demonstrated higher NPQ under low light but also obtained the greatest magnitude of change in NPQ from 100 to 1000 μmol m^{-2} s^{-1} PPFD (Fig. S5).

The kinetics of NPQ in response to changes in irradiance are indicative of the dynamic equilibrium between photoprotection and photochemistry in response to the fluctuating light environment experienced in the field. The analysis presented here indicates interesting and accession-dependent trends in the speed of NPQ induction and relaxation. For example, the time taken to induce 50% of the maximum NPQ under 1000 μmol m^{-2} s^{-1} PPFD (I_{50}; Fig. 5a) was consistently lower than the time taken to relax to 50% minimum NPQ under 100 μmol m^{-2} s^{-1} PPFD (R_{50}; Fig. 5b) for all accessions. Interestingly, there was no correlation observed between I_{50} and R_{50} ($R^2 = -0.06$, $P = 0.80$).

In general, although there were significant accession-specific differences in I_{50} ($P < 0.0001$) and R_{50} ($P < 0.0001$), the range of I_{50} (1.9–7 s) was much narrower than that observed for R_{50} (26–133 s). In general, the wild *Triticum* species took the least time to induce (2.13 ± 0.43 s), whereas the modern *Triticum* took the longest (5.34 ± 1.25 s). By contrast, the modern *Triticum* achieved the fastest R_{50} time (79.32 ± 20.61 s),

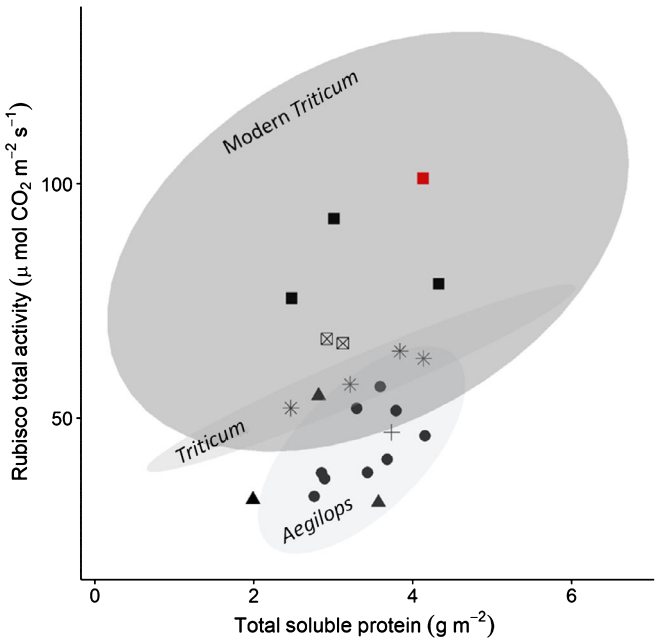

Fig. 4 Total soluble protein and Rubisco total activity was determined from the flag leaves of three modern *Triticum* (black squares) varieties and 19 wild relative species across five genera: *Aegilops* (red circles), *Ambylopyrum* (black triangles), *Secale* (black plus symbols), *Triticum* (black asterisks), and *Thinopyrum* (black enclosed crosses). The modern cultivar, *Triticum aestivum* 'Paragon', is highlighted (red square), and ellipses highlight the largest genus groups modern *Triticum*, *Triticum* and *Aegilops*. Data are the means (n = 2–5 biological replicates).

whereas the *Thinopyrum* species took the longest to relax (111.02 ± 19.73 s). We conclude that modern wheat has faster NPQ relaxation than the wild relatives do with a slower induction. Some genus outliers were noted; for example, *Aegilops biuncialis* 550945 and *Triticum monococcum* took respectively 2.7 and 1.5-fold longer to induce NPQ than the other *Aegilops* and *Triticum* species did. On average, *Triticum timopheevii* took 245 s to relax to 50% minimum NPQ, compared with the *Triticum* average of 70 s. Interestingly, those plants with a faster NPQ induction might have a higher capacity for photosynthesis: a significant negative relationship was observed between A_{max} and I_{50} (Fig. 6a; $R^2 = -0.46$, $P < 0.03$), whereas no correlation was observed between A_{max} and R_{50} (Fig. 6b; $R^2 = 0.01$, $P = 0.96$).

Stomatal dynamics

Stomatal responses are an order of magnitude slower than metabolic processes. To investigate variation in stomatal responses, 24 accessions were subjected to a step increase in PPFD from 100 to 1000 μmol m^{-2} s^{-1} PPFD and a model used to determine both magnitude of opening and rapidity of response (Vialet-Chabrand *et al.*, 2013). Substantial variation in dynamics of stomata was observed among the wild relatives, with some faster than the modern wheat. At steady state, no significant correlation ($R^2 = -0.05$, $P = 0.81$) was determined between A and g_s under 1000 μmol m^{-2} s^{-1} PPFD (A_{1000} and g_{s1000}, respectively; Fig. 7a). In addition, no correlation was observed between g_{s1000} and g_s under 100 μmol m^{-2} s^{-1} PPFD ($R^2 = 0.14$) or between A_{1000} and A_{max} ($R^2 = 0.02$, $P = 0.93$).

A significant positive relationship ($R^2 = 0.87$, $P < 0.0001$) was observed for the time taken to achieve 95% A_{1000} and g_{s1000} (Fig. 7b); however, all species took longer to achieve 95% g_{s1000} compared with 95% A_{1000}. Those species that took the longest to achieve 95% A_{1000} also achieved higher A_{1000} values ($R^2 = 0.41$, $P < 0.05$), with the modern *Triticum* accessions achieving the highest A_{1000} values (19.9 ± 2.1 μmol m^{-2} s^{-1}), on average 2.8 ± 0.6 μmol m^{-2} s^{-1} greater than the other five genera measured. The species achieving the highest mean A_{1000} for the lowest mean g_{s1000} – and hence the highest intrinsic water-use efficiency (W_i, μmol CO_2 $mmol^{-1}$ H_2O m^{-2} s^{-1}) – was *T. monococcum* TM01 (0.044 μmol CO_2 $mmol^{-1}$ H_2O m^{-2} s^{-1}), whereas the lowest W_i was found for *Aeglps caudata* 2090001 (0.022 μmol CO_2 $mmol^{-1}$ H_2O m^{-2} s^{-1}).

On average, the stomata from *Thinopyrum* accessions were the fastest (6.1 ± 1.3 min) to achieve 95% A_{1000}, whereas the *Aegilops* accessions were the slowest (8.6 ± 1.5 min). To achieve 95% g_{s1000}, all species opened for an average of 7.0 min (± 2.3 min) longer than was required to achieve 95% A_{1000}. The longest time was found in *S. cereale* 428373, which achieved 95% g_{s1000} *c.* 4 min later than the other genera (11.0 min). There was no correlation between the maximum rate of g_s increase to a doubling in PPFD from 100 to 1000 μmol m^{-2} s^{-1} (Sl_{max}) and the time constant used to describe the time taken to achieve steady-state g_s (k) and A_{1000} ($R^2 = -0.14$, $P = 0.51$ and $R^2 = 0.19$, $P = 0.37$, respectively). To relate speed with magnitude of opening, Sl_{max} and k were compared with g_{s1000}; whereas a positive correlation was observed between Sl_{max} and g_{s1000} ($R^2 = 0.60$, $P = 0.01$), no correlation was observed between k and g_{s1000} ($R^2 = -0.04$, $P = 0.85$).

Finally, when comparing across experiments, a significant positive correlation was observed between Sl_{max} and NPQ under 1000 μmol m^{-2} s^{-1} PPFD (NPQ_{1000}, $R^2 = 0.52$, $P = 0.03$) and between g_{s1000} and I_{50} ($R^2 = 0.48$, $P = 0.05$). Interestingly, a positive relationship was determined between A_{1000} and I_{50} ($R^2 = 0.65$, $P = 0.005$), whereas a negative correlation was seen between A_{1000} and NPQ_{1000} ($R^2 = -0.50$, $P = 0.04$).

Whole plant and leaf characteristics

Leaf morphological analysis was carried out on a selection of the accessions (25 wild relative accessions and three modern genotypes; Figs S6–S9). Though we do not expect yield components to be of value in the undomesticated species, we note some interesting relationships relevant to the theme of this paper. There was a genus-specific negative correlation between SLA and A_{max} (Fig. S6), suggesting a functional trade-off between leaf thickness, density of photosynthetic components, and photosynthetic capacity. We also noted negative correlations between SLA (Fig. S7a), leaf absorbance (Fig. S8, $R^2 = -0.50$, $P = 0.03$), and total Rubisco activity ($R^2 = -0.49$, $P = 0.04$). A positive correlation was also observed between SLA and ear number (Fig. S9; $R^2 = 0.70$, $P = 0.0001$).

The *Aegilops* accessions were found to have the highest SLA (Fig. S7a; $P < 0.003$), whereas *Thinopyrum* had the lowest ($P <$

New Phytologist

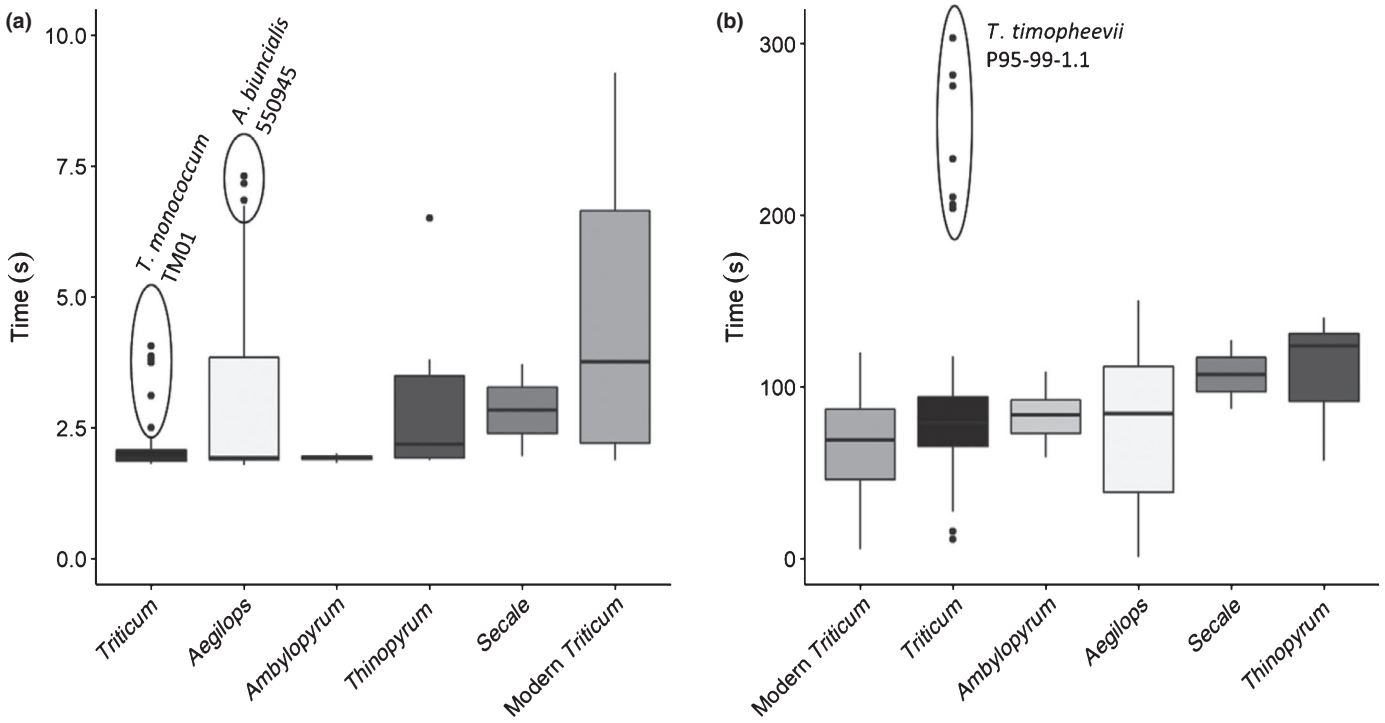

Fig. 5 Time taken to (a) induce (I_{50}) and (b) relax (R_{50}) nonphotochemical quenching to 50% of maximum under 1000 μmol m^{-2} s^{-1} photosynthetic photon flux density (PPFD) and 100 μmol m^{-2} s^{-1} PPFD, respectively, in five genera. Outlying species are circled and annotated. The data are the means (n = 3–17 biological replicates). Boxplots show the median (horizontal line) and the quartiles (boxes). The whiskers represent 1.5-times the interquartile range above and below the 75th and 25th percentiles, respectively, with extreme values indicated as dots.

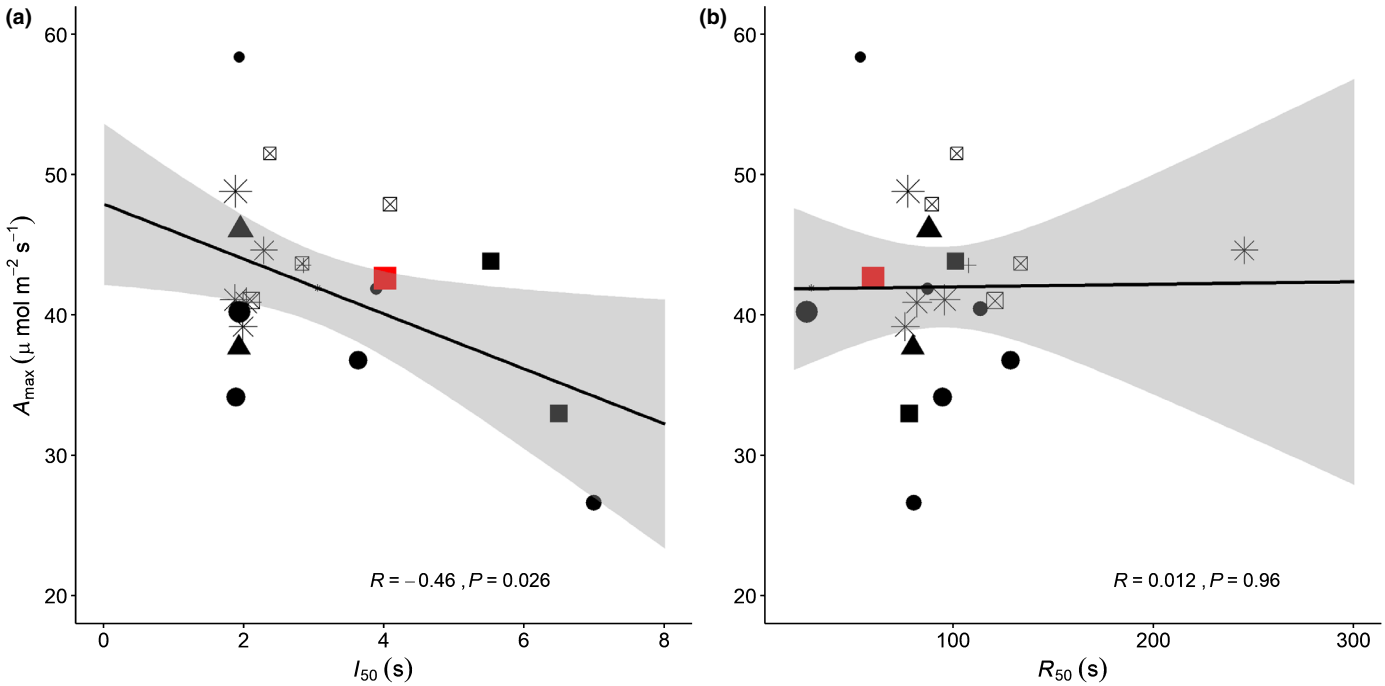

Fig. 6 The relationship between CO_2 and light-saturated rates of photosynthetic assimilation A_{max} and (a) the time taken to achieve 50% maximum nonphotochemical quenching (NPQ) under 1000 μmol m^{-2} s^{-1} photosynthetic photon flux density (PPFD) and (b) the time taken to achieve 50% minimum NPQ under 100 μmol m^{-2} s^{-1} PPFD. Data are the mean for each species (n = 3–18), with genus indicated by shape: modern *Triticum* (black squares), *Aegilops* (black circles), *Ambylopyrum* (black triangles), *Secale* (black plus symbols), *Triticum* (black asterisks), and *Thinopyrum* (black enclosed crosses). The modern cultivar, *Triticum aestivum* 'Paragon', is highlighted (red squares). The larger the data point the greater the value of NPQ achieved under 1000 μmol m^{-2} s^{-1} PPFD. A linear regression is fitted to all data, with the shading indicating a 95% confidence interval on the fitted values. A Pearson's correlation coefficient is shown in the bottom right corner of each plot.

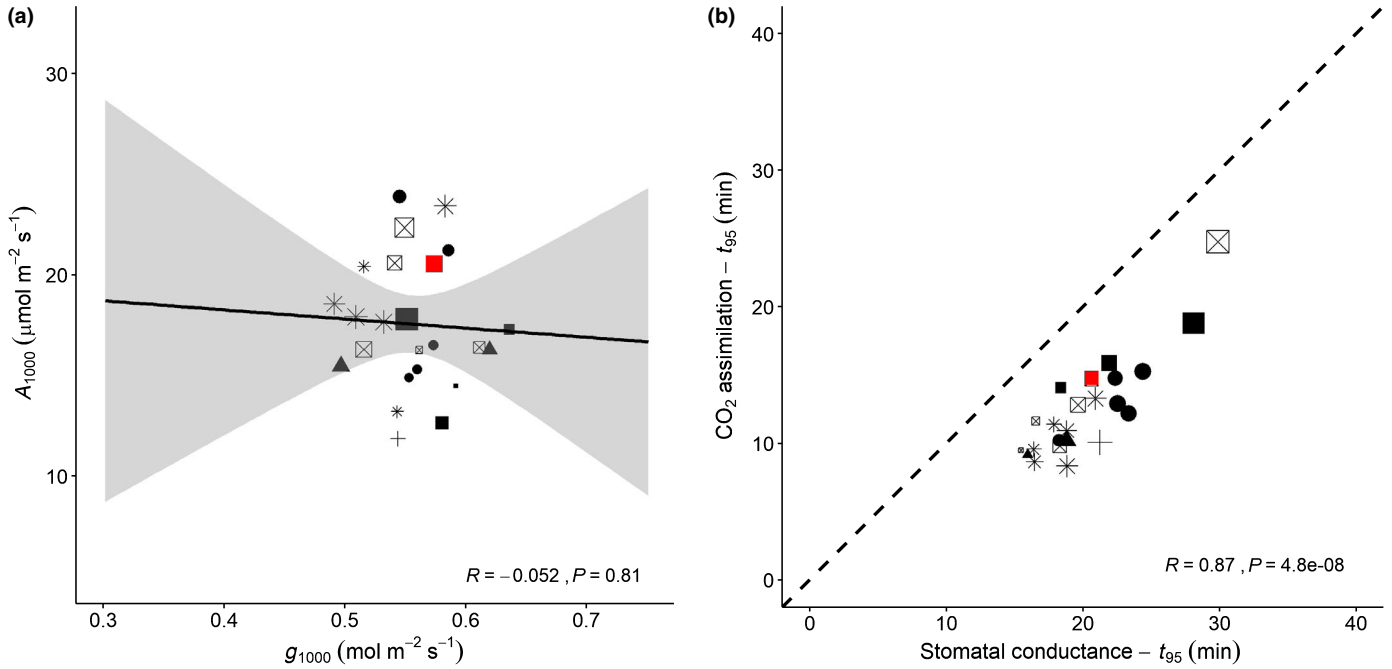

Fig. 7 (a) The relationship between maximum stomatal conductance g_{1000} and CO_2 assimilation A_{1000} under 1000 μmol m^{-2} s^{-1} PPFD. (b) To highlight stomatal limitation on CO_2 assimilation between species, the relationship between the times taken to achieve 95% (t_{95}) of A_{1000} and g_{1000} under 1000 μmol m^{-2} s^{-1} photosynthetic photon flux density are plotted and a 1 : 1 relationship is indicated (dashed line). For both plots, data are the mean for each species, with genus indicated by shape: modern *Triticum* (black squares), *Aegilops* (black circles), *Ambylopyrum* (black triangles), *Secale* (black plus symbols), *Triticum* (black asterisks), and *Thinopyrum* (black enclosed crosses). The modern cultivar, *Triticum aestivum* 'Paragon', is highlighted (red squares). For plot (a), the larger the data point the greater the time taken to achieve 95% A_{1000}; for plot (b), the larger the shape the greater the time constant used to describe the time taken for stomata to open (k) and a selection of accessions are labelled. A linear regression is fitted to all data points, with the shading indicating a 95% confidence interval on the fitted values. A Pearson's correlation coefficient is shown in the bottom right corner of each plot.

0.03). With the exception of *T. timopheevii* P9599.11 (34.3 ± 6.4%), the wild *Triticum* accessions were found to have the highest percentage DW (Fig. S7b; 77.0 ± 14.0%), whereas modern *Triticum* and *Secale* exhibited the lowest (27.1 ± 1.4% and 30.5 ± 1.4%, respectively). Unsurprisingly, modern *Triticum* flag leaves absorbed the highest percentage of light (86.3 ± 1.9%; Fig. S8) – significantly ($P < 0.05$) greater than wild *Triticum* (83.2 ± 1.9%), *Aegilops* (81.1.3 ± 3.0%), and *Amblyopyrum* (80.7 ± 2.3%) genera. When illuminated under 2000 μmol m^{-2} s^{-1} PPFD, this variation in flag leaf absorbance accounted for between 280 and 400 μmol m^{-2} s^{-1} PPFD not utilized for C gain.

Discussion

Physiological and genotypic exploration of variation associated with the improvement of photosynthesis is crucial for the successful introduction and identification of interrelated traits that improve biomass acquisition in staple crops such as wheat and rice. Using wild relatives to introduce new genetic diversity into elite cultivars has gathered momentum in recent years (King *et al.*, 2017; Prohens *et al.*, 2017), generating a need for understanding the breadth of physiological variation available to breeding programmes, particularly traits that promote greater C acquisition. Here, we address this for the first time and encompass a wide selection of notable wild relatives, originating from > 14 countries, covering 35 polyploid genomes, six genera, and 37 genetically distinct species (Fig. 1; Table S2). We have provided a database of photosynthetic traits, shown substantial variation for key photosynthetic traits, and discovered novel patterns among the wild relatives that partly explain the underlying causes of the differences observed.

Our results suggest that highly significant variation exists between the six genera, both for the capacity to fix CO_2 under saturating conditions (Figs 2–4) and for temporal processes that facilitate the achievement of high rates of CO_2 uptake under fluctuating conditions, such as those found in the field. High flag-leaf photosynthesis can be correlated to grain yield in modern wheat cultivars (Fischer *et al.*, 1998; Gaju *et al.*, 2016; Carmo-Silva *et al.*, 2017). This is often linked to Rubisco activity. Curiously, though Rubisco total activity was found to be highest in the modern cultivars, the high A_{max} values observed in the wild relative genera were underpinned by higher and wider ranges of maximum carboxylation V_{cmax} and electron transport J_{max}. In addition, the wild relative genera exhibited greater J_{max} : V_{cmax} ratios, driven by higher values of J_{max} (and hence the electron-transport-mediated rate of RuBP regeneration; Fig. 3). Whereas some accessions (such as *Aegilops juvenalis* 574463 (#1), *Thinopyrum ponticum* 547312 (#70) and *T. dicoccoides* P95983.2 (#76)) utilized this relationship for increased rates of C uptake, some accessions (e.g. *Aegilops biuncialis* 550940 (#29)) still achieved high J_{max} : V_{cmax} ratios without the accompanying increase in A_{max}. Therefore, there is broad lack of tightness between carboxylation

capacity and electron transport capacity across the material analysed here. However, J_{max} values estimated from A vs C_i analyses may not always accurately represent maximum electron transport rate (Buckley & Diaz-Espejo, 2015). Calculation of $C_{itransition}$ indicates the likely point for limitation of CO_2 assimilation (i.e. RuBP carboxylation or regeneration) and also indicates N partitioning among photosynthetic components (Yamori *et al.*, 2011). Greater leaf N content may decrease the V_{cmax} : J_{max} (Yamori *et al.*, 2011); therefore, it is possible that some variation could be explained by differences in N investment between electron transport and Rubisco. To support this, modern lines in the current study had the lowest $C_{itransition}$ (Figs 3, S2b). Higher Rubisco activity in modern varieties is not a surprise since it would be expected that these genotypes would take up and accumulate a higher leaf N content for ready mobilization from leaf to the grain during senescence (Havé *et al.*, 2017).

We speculate that the higher V_{cmax} in some wild relatives may be related to possession of thick, narrow leaves (a tendency in some lines), which is supported by the negative relationship between A_{max} and SLA (Fig. S6). Quantifying variation in V_{cmax} and J_{max} is vital in modelling C exchange at different scales (Rogers *et al.*, 2017; Bloomfield *et al.*, 2019) and is mediated by the balance of leaf N and phosphate, often evidenced by changes in SLA (Reich *et al.*, 1997; Evans & Poorter, 2001). Though changes in SLA can alter the N content per unit leaf area, they can also change the light absorbance of the leaf, with decreases in J_{max} being somewhat negated by increases in absorbance (Evans & Poorter, 2001). The modern cultivars in this study had some of the lowest electron transport rates but also achieved some of the highest absorbance values, accompanied by low SLA (Figs S1, S7a, S8).

It should also be noted that increases in J_{max} (such as those observed for the wild relatives) are not always directly associated with improvements in CO_2 uptake by the Calvin–Benson cycle. With high electron transport rates increasing the reducing power for other essential pathways in the leaf, such as chloroplastic conversion of nitrate to ammonium (Anderson & Done, 1978; Searles & Bloom, 2003), driving production of isoprene (Morfopoulos *et al.*, 2013), and driving alternative electron sinks, such as the Mehler reaction, reflecting changes in the apportionment of photosynthetic proteins (Yamori *et al.*, 2005). Changes in the V_{cmax} to J_{max} ratio may also reflect the resource allocation bias of the plant to maintain high photosynthetic rates to set down biomass and remain competitive (Bryant *et al.*, 1998), with leaves at the top of the canopy limited by V_{cmax} rather than J_{max} at ambient CO_2 (Quebbeman & Ramirez, 2016).

Walker *et al.* (2014) modelled the instantaneous relationship between J_{max} and V_{cmax} under fluctuating light, hypothesizing that increases in J_{max} compensated for Rubisco carboxylation limitations under high light, thus increasing photoprotection and buffering against photoinhibition (Walker *et al.*, 2014). By contrast, the work presented here showed NPQ_{1000} was highest in modern *Triticum* and wild *Triticum* genera (Fig. S5), despite the lower J_{max} values. Interestingly, the modern cultivars also demonstrated some of the slowest rates of NPQ induction (I_{50}; Fig. 5a). This suggests that higher rates of electron transport supported faster induction in a handful of wild relatives but not greater magnitudes of photoprotection under high light conditions (Fig. S5).

Manipulating photoprotection is another route for increasing yield, and through identifying and manipulating the magnitude and response timings of NPQ this has led to improvements in crop productivity (Hubbart *et al.*, 2012; Kromdijk *et al.*, 2016). Interestingly, 18 of the 24 wild relative accessions responded faster than the modern cultivar 'Paragon' to a step increase in PPFD, which suggests there may be some room to improve NPQ induction and relaxation in this modern cultivar. The significant negative correlation between A_{max} and I_{50} is a strong example of screening for a temporal trait that can be linked with improvements in photosynthetic capacity. In rice, fast induction of NPQ was linked to an inhibition of the rise in CO_2 assimilation (Hubbart *et al.*, 2012), consistent with this trend. Furthermore, these data suggest that I_{50} could be utilized as a proxy for the more time-intensive measurements of A_{max}, allowing greater numbers of plants to be screened more rapidly for variation in photosynthetic capacity (McAusland *et al.*, 2019).

Decreasing the relaxation time could be advantageous for leaves constantly under rapid high light fluctuations, allowing efficient induction of photosynthesis to maximally utilize available PPFD (Murchie & Niyogi, 2011; Murchie & Ruban, 2019). A much greater range of R_{50} values was observed between the accessions than with the I_{50} values. Though there was no correlation between A_{max} and R_{50}, this does not mean that the rate of relaxation is not important in C acquisition. Instead, it has been shown to be important during fluctuations in PPFD, and, if reduced, it could increase C fixation 7–30% during a diurnal time course (Long *et al.*, 1994; Werner *et al.*, 2001; Zhu *et al.*, 2004; Kromdijk *et al.*, 2016). In general, the modern cultivars took the shortest time to relax NPQ, but there were examples of specific wild relative accessions that relaxed more rapidly (Fig. 5b).

Stomatal behaviour is another temporal trait that has been the focus of recent work on optimizing the balance between C gained and water lost (Lawson & Vialet-Chabrand, 2019). I_{50} was found to positively correlate with the magnitude of stomatal opening g_{s1000} and CO_2 assimilation rates achieved under 1000 μmol m^{-2} s^{-1} PPFD (A_{1000}), highlighting that greater opening not only allows higher A_{1000} but also facilitates more rapid induction of NPQ under high light. These data suggest that, under high light, the plant mediates a fine balance between maintaining high rates of carbon fixation, with subsequent induction of photoprotection, and minimizing loss of water. Interestingly, there was no correlation between g_{s1000} and A_{1000}, suggesting that the variation observed in g_{s1000} could be manipulated to reduce water loss without restricting C gain – exemplified by the two-fold difference in W_i values between the accessions measured (Fig. 7b).

Though large variation in the rate of stomatal opening has been observed between different species (McAusland *et al.*, 2016) and between cultivars of a single species (Faralli *et al.*, 2019a), the total time taken to achieve steady-state g_s (k) has been shown not to correlate with maximum opening under high light (Vialet-

Chabrand *et al.*, 2013; McAusland *et al.*, 2016). Maximum rate of opening Sl_{max} is mathematically dependent on the magnitude of change in g_s (k) and maximum opening, and therefore it is not unsurprising that those species that achieved greater g_{s1000} also achieved the highest Sl_{max}. However, the variation in maximum opening is somewhat determined by the stomatal density : size relationship (Franks & Beerling, 2009). These data point to anatomical variability between the wild relative accessions; and though densities in modern cultivars are known to have increased through breeding (Fischer *et al.*, 1998), there may still be an optimal density for minimizing water loss evidenced by a wild relative genus or accession. Maintaining high water-use efficiency is a particularly relevant target for modern cultivars, which typically exhibit a higher leaf water content than wild relative species (Fig. S7b). In addition, efficient water management will directly contribute to improved tolerance to drought and heat stress, therefore maintaining yields under increasing unpredictable climactic conditions (Bertolino *et al.*, 2019).

As with stomatal density, internal leaf anatomy will also contribute to the photosynthetic variation discovered in this study; with traits such as airspace volume (Lehmeier *et al.*, 2017), mesophyll size (Austin *et al.*, 1982), porosity and conductance (Lundgren *et al.*, 2019), and distance to veins (Brodribb *et al.*, 2007) playing a vital role in efficient C acquisition. Though no anatomical measurements are presented in this study, the significant variation in SLA (Fig. S7a) and absorbance (Fig. S8) suggests that extensive variation occurs at the cellular level.

It is important that both static and temporal responses are measured so that the capacity, dynamic adaptability, and the interrelated nature of the processes that support and maintain high rates of C acquisition are identified (Murchie *et al.*, 2018; Lawson & Vialet-Chabrand, 2019; Salter *et al.*, 2019). Methodologies such as the Chl fluorescence screen described here (McAusland *et al.*, 2019), and other powerful platforms (e.g. Vialet-Chabrand & Lawson, 2019, 2020), offer rapid, high detail measurements that can be taken during the lifetime of the plant rather than at single phenological stages. Here, we cultivated plants in glasshouse conditions but note the importance of further studies in variable field-like conditions (Poorter *et al.*, 2016). However, A_{max} values for 'Paragon' are similar to those observed by Driever *et al.* (2014), a field-based study. Complex emerging data sets may require development of functional models to predict optimal combinations in realistic field environments (e.g. Zhu *et al.*, 2012; Wu *et al.*, 2019).

Though only briefly mentioned here, the wild relatives of modern wheat also demonstrate a wealth of variation in agronomically important traits, such as disease (Table S1) and biotic resistance (Peleg *et al.*, 2005), phenology (e.g. flowering time, perennial or annual), pollen fecundity, and root physiology (de Dorlodot *et al.*, 2007; Atkinson, 2016). Quantifying and understanding the breadth of diversity available, tempered by the ease of introducing the material into modern wheat backgrounds, will not only enable efficient strategic crosses in breeding programmes designed to improve photosynthetic C gain but also provide traits to screen for in the subsequent backcross generations. In turn, this will speed up the identification of direct and related phenotypes associated with increased C assimilation per unit area, leading to greater biomass and improved yield.

Concluding remarks

The wild relatives of crop species represent a way of targeted introduction of beneficial traits to improve yield. Until now, photosynthetic variation in the wild relatives of wheat has not been explored. Here, we analyse relevant features of static and dynamic traits across a broad range of wild accessions and genera. The widest variation was found across individual accessions, suggesting local adaptation to be important when selecting crosses and that genotyping of individual accessions is important. We find key differences between wild relatives and modern lines for dynamic traits, notably that photoprotection relaxation is fast in modern lines but induction is slow. These results highlight fundamental variation in wild species and those that may have indirectly been selected for in breeding. The phenotypic and genotypic data presented are a first step to inform follow-on gene discovery and pre-breeding programmes.

Acknowledgements

This work was funded by the Biotechnology and Biological Research Council (grant no. BB/N021061/1) and carried out as part of the International Wheat Yield Partnership (IWYP). We thank Dr Kai Sonder, Dr Carolina Rivera-Amado, and Gilberto Thompson-Valencia (CIMMYT) for their help compiling the map of the mega-environments shown in Fig. 1. We also thank Laura Briers and Tim Chisnall for their help during this project.

Author contributions

EHM, KJE, JK, IPK, ECS and TL planned and designed the research. SHE and KP contributed to the planning of the research. LM, SVC, AB, MJF and IJ performed experiments and analysed data. LM and EHM wrote the manuscript with input from the other authors.

ORCID

Amanda Burridge https://orcid.org/0000-0002-0140-5523
Elizabete Carmo-Silva https://orcid.org/0000-0001-6059-9359
Keith J. Edwards https://orcid.org/0000-0002-5776-5798
Stella Hubbart-Edwards https://orcid.org/0000-0002-9286-154X
Iván Jauregui https://orcid.org/0000-0002-6958-6746
Ian P. King https://orcid.org/0000-0001-7017-0265
Julie King https://orcid.org/0000-0002-7699-7199
Tracy Lawson https://orcid.org/0000-0002-4073-7221
Lorna McAusland https://orcid.org/0000-0002-5908-1939
Erik H. Murchie https://orcid.org/0000-0002-7465-845X
Kevin Pyke https://orcid.org/0000-0003-0604-6088
Silvere Vialet-Chabrand https://orcid.org/0000-0002-2105-2825

References

Anderson JW, Done J. 1978. Light-dependent assimilation of nitrite by isolated pea chloroplasts. *Plant Physiology* **61**: 692–697.

Araus JL, Kefauver SC, Zaman-Allah M, Olsen MS, Cairns JE. 2018. Translating high-throughput phenotyping into genetic gain. *Trends in Plant Science* **23**: 451–466.

Atkinson JA. 2016. *Phenotyping root architecture in diverse wheat germplasm.* PhD thesis, University of Nottingham, Nottingham, UK.

Austin R, Morgan C, Ford M, Bhagwat S. 1982. Flag leaf photosynthesis of *Triticum aestivum* and related diploid and tetraploid species. *Annals of Botany* **49**: 177–189.

Baker NR. 2008. Chlorophyll fluorescence: a probe of photosynthesis *in vivo*. *Annual Review of Plant Biology* **59**: 89–113.

Bertolino LT, Caine RS, Gray JE. 2019. Impact of stomatal density and morphology on water-use efficiency in a changing world. *Frontiers in Plant Science* **10**: e225.

Bloomfield KJ, Prentice IC, Cernusak LA, Eamus D, Medlyn BE, Rumman R, Wright IJ, Boer MM, Cale P, Cleverly J *et al.* 2019. The validity of optimal leaf traits modelled on environmental conditions. *New Phytologist* **221**: 1409–1423.

Bradford MM. 1976. A rapid and sensitive method for the quantitation of microgram quantities of protein utilizing the principle of protein-dye binding. *Analytical Biochemistry* **72**: 248–254.

Brisson N, Gate P, Gouache D, Charmet G, Oury F-X, Huard F. 2010. Why are wheat yields stagnating in Europe? A comprehensive data analysis for France. *Field Crops Research* **119**: 201–212.

Brodribb TJ, Feild TS, Jordan GJ. 2007. Leaf maximum photosynthetic rate and venation are linked by hydraulics. *Plant Physiology* **144**: 1890–1898.

Bryant J, Taylor G, Frehner M. 1998. Photosynthetic acclimation to elevated CO_2 is modified by source : sink balance in three component species of chalk grassland swards grown in a free air carbon dioxide enrichment (FACE) experiment. *Plant, Cell & Environment* **21**: 159–168.

Buckley TN, Diaz-Espejo A. 2015. Reporting estimates of maximum potential electron transport rate. *New Phytologist* **205**: 14–17.

Burgess AJ, Retkute R, Pound MP, Foulkes J, Preston SP, Jensen OE, Pridmore TP, Murchie EH. 2015. High-resolution three-dimensional structural data quantify the impact of photoinhibition on long-term carbon gain in wheat canopies in the field. *Plant Physiology* **169**: 1192–1204.

Burt C, Nicholson P. 2011. Exploiting co-linearity among grass species to map the *Aegilops ventricosa*-derived *Pch1* eyespot resistance in wheat and establish its relationship to *Pch2*. *Theoretical and Applied Genetics* **123**: 1387–1400.

Carmo-Silva E, Andralojc PJ, Scales JC, Driever SM, Mead A, Lawson T, Raines CA, Parry MA. 2017. Phenotyping of field-grown wheat in the UK highlights contribution of light response of photosynthesis and flag leaf longevity to grain yield. *Journal of Experimental Botany* **68**: 3473–3486.

Carmo-Silva E, Scales JC, Madgwick PJ, Parry MA. 2015. Optimizing Rubisco and its regulation for greater resource use efficiency. *Plant, Cell & Environment* **38**: 1817–1832.

Charmet G. 2011. Wheat domestication: lessons for the future. *Comptes Rendus Biologies* **334**: 212–220.

Chen G, Zheng Q, Bao Y, Liu S, Wang H, Li X. 2012. Molecular cytogenetic identification of a novel dwarf wheat line with introgressed *Thinopyrum ponticum* chromatin. *Journal of Biosciences* **37**: 149–155.

Cornelissen JHC, Lavorel S, Garnier E, Díaz S, Buchmann N, Gurvich DE, Reich PB, ter Steege H, Morgan HD, van der Heijden MGA *et al.* 2003. A handbook of protocols for standardised and easy measurement of plant functional traits worldwide. *Australian Journal of Botany* **51**: 335–380.

de Dorlodot S, Forster B, Pagès L, Price A, Tuberosa R, Draye X. 2007. Root system architecture: opportunities and constraints for genetic improvement of crops. *Trends in Plant Science* **12**: 474–481.

Devi U, Grewal S, Yang C-y, Hubbart-Edwards S, Scholefield D, Ashling S, Burridge A, King IP, King J. 2019. Development and characterisation of interspecific hybrid lines with genome-wide introgressions from *Triticum timopheevii* in a hexaploid wheat background. *BMC Plant Biology* **19**: e183.

Dixon J, Braun H-J, Kosina P, Crouch JH eds. 2009. *Wheat facts and futures 2009.* CIMMYT Facts and Trends. Mexico City, Mexico: CIMMYT.

Doussinault G, Delibes A, Sanchez-Monge R, Garcia-Olmedo F. 1983. Transfer of a dominant gene for resistance to eyespot disease from a wild grass to hexaploid wheat. *Nature* **303**: 698–700.

Driever S, Lawson T, Andralojc P, Raines C, Parry M. 2014. Natural variation in photosynthetic capacity, growth, and yield in 64 field-grown wheat genotypes. *Journal of Experimental Botany* **65**: 4959–4973.

Driever SM, Simkin AJ, Alotaibi S, Fisk SJ, Madgwick PJ, Sparks CA, Jones HD, Lawson T, Parry MA, Raines CA. 2017. Increased SBPase activity improves photosynthesis and grain yield in wheat grown in greenhouse conditions. *Philosophical Transactions of the Royal Society B: Biological Sciences* **372**: e20160384.

Duursma RA. 2015. PLANTECOPHYS – an R package for analysing and modelling leaf gas exchange data. *PLoS ONE* **10**: e0143346.

Evans JR, Lawson T. 2020. From green to gold: agricultural revolution for food security. *Journal of Experimental Botany.* **71**: 2211–2215.

Evans J, Poorter H. 2001. Photosynthetic acclimation of plants to growth irradiance: the relative importance of specific leaf area and nitrogen partitioning in maximizing carbon gain. *Plant, Cell & Environment* **24**: 755–767.

Faralli M, Cockram J, Ober E, Wall S, Galle A, Van Rie J, Raines CA, Lawson T. 2019a. Genotypic, developmental and environmental effects on the rapidity of g_s in wheat: impacts on carbon gain and water-use efficiency. *Frontiers in Plant Science* **10**: e492.

Faralli M, Matthews J, Lawson T. 2019b. Exploiting natural variation and genetic manipulation of stomatal conductance for crop improvement. *Current Opinion in Plant Biology* **49**: 1–7.

Faris JD. 2014. Wheat domestication: key to agricultural revolutions past and future. In: Tuberosa R, Graner A, Frison E, eds. *Genomics of plant genetic resources*. Dordrecht, the Netherlands: Springer, 439–464.

Farquhar GD, von Caemmerer S, Berry JA. 1980. A biochemical model of photosynthetic CO_2 assimilation in leaves of C_3 species. *Planta* **149**: 78–90.

Fischer R, Rees D, Sayre K, Lu Z-M, Condon A, Saavedra AL. 1998. Wheat yield progress associated with higher stomatal conductance and photosynthetic rate, and cooler canopies. *Crop Science* **38**: 1467–1475.

Franks PJ, Beerling DJ. 2009. Maximum leaf conductance driven by CO_2 effects on stomatal size and density over geologic time. *Proceedings of the National Academy of Sciences, USA* **106**: 10343–10347.

Gaju O, DeSilva J, Carvalho P, Hawkesford MJ, Griffiths S, Greenland A, Foulkes MJ. 2016. Leaf photosynthesis and associations with grain yield, biomass and nitrogen-use efficiency in landraces, synthetic-derived lines and cultivars in wheat. *Field Crops Research* **193**: 1–15.

Global Diversity Trust. 2019. Wheat: *Triticum* spp. [WWW document] URL https://www.cwrdiversity.org/crop/wheat/ [accessed 9 July 2019].

Grewal S, Edwards SH, Yang C, Scholefield D, Ashling S, Burridge A, Wilkinson PA, King IP, King J. 2018a. Detection of *T. urartu* introgressions in wheat and development of a panel of interspecific introgression lines. *Frontiers in Plant Science* **9**: e1565.

Grewal S, Hubbart-Edwards S, Yang C, Devi U, Baker L, Heath J, Ashling S, Scholefield D, Howells C, Yarde J. 2020. Rapid identification of homozygosity and site of wild relative introgressions in wheat through chromosome-specific KASP genotyping assays. *Plant Biotechnology Journal* **18**: 743–755.

Grewal S, Yang C, Edwards SH, Scholefield D, Ashling S, Burridge AJ, King IP, King J. 2018b. Characterisation of *Thinopyrum bessarabicum* chromosomes through genome-wide introgressions into wheat. *Theoretical and Applied Genetics* **131**: 389–406.

Havé M, Marmagne A, Chardon F, Masclaux-Daubresse C. 2017. Nitrogen remobilization during leaf senescence: lessons from Arabidopsis to crops. *Journal of Experimental Botany* **68**: 2513–2529.

Hubbart S, Ajigboye OO, Horton P, Murchie EH. 2012. The photoprotective protein PsbS exerts control over CO_2 assimilation rate in fluctuating light in rice. *The Plant Journal* **71**: 402–412.

King IP, Forster BP, Law CC, Cant KA, Orford SE, Gorham J, Reader S, Miller TE. 1997. Introgression of salt-tolerance genes from *Thinopyrum bessarabicum* into wheat. *New Phytologist* **137**: 75–81.

King J, Grewal S, Yang C-Y, Hubbart Edwards S, Scholefield D, Ashling S, Harper JA, Allen AM, Edwards KJ, Burridge AJ *et al.* 2018. Introgression of

Aegilops speltoides segments in *Triticum aestivum* and the effect of the gametocidal genes. *Annals of Botany* **121**: 229–240.

King J, Grewal S, Yang CY, Hubbart S, Scholefield D, Ashling S, Edwards KJ, Allen AM, Burridge A, Bloor C. 2017. A step change in the transfer of interspecific variation into wheat from *Amblyopyrum muticum*. *Plant Biotechnology Journal* **15**: 217–226.

Kromdijk J, Głowacka K, Leonelli L, Gabilly ST, Iwai M, Niyogi KK, Long SP. 2016. Improving photosynthesis and crop productivity by accelerating recovery from photoprotection. *Science* **354**: 857–861.

Lawson T, Blatt M. 2014. Stomatal size, speed and responsiveness impact on photosynthesis and water use efficiency. *Plant Physiology* **164**: 1556–1570.

Lawson T, Vialet-Chabrand S. 2019. Speedy stomata, photosynthesis and plant water use efficiency. *New Phytologist* **221**: 93–98.

Lehmeier C, Pajor R, Lundgren MR, Mathers A, Sloan J, Bauch M, Mitchell A, Bellasio C, Green A, Bouyer D. 2017. Cell density and airspace patterning in the leaf can be manipulated to increase leaf photosynthetic capacity. *The Plant Journal* **92**: 981–994.

Long SP, Humphries S, Falkowski PG. 1994. Photoinhibition of photosynthesis in nature. *Annual Review of Plant Biology* **45**: 633–662.

Long SP, Zhu XG, Naidu SL, Ort DR. 2006. Can improvement in photosynthesis increase crop yields? *Plant, Cell & Environment* **29**: 315–330.

Lundgren MR, Mathers A, Baillie AL, Dunn J, Wilson MJ, Hunt L, Pajor R, Fradera-Soler M, Rolfe S, Osborne CP. 2019. Mesophyll porosity is modulated by the presence of functional stomata. *Nature Communications* **10**: e2825.

Maxwell K, Johnson GN. 2000. Chlorophyll fluorescence – a practical guide. *Journal of Experimental Botany* **51**: 659–668.

McAusland L, Atkinson JA, Lawson T, Murchie EH. 2019. High throughput procedure utilising chlorophyll fluorescence imaging to phenotype dynamic photosynthesis and photoprotection in leaves under controlled gaseous conditions. *Plant Methods* **15**: e109.

McAusland L, Vialet-Chabrand S, Davey P, Baker NR, Brendel O, Lawson T. 2016. Effects of kinetics of light-induced stomatal responses on photosynthesis and water-use efficiency. *New Phytologist* **211**: 1209–1220.

McAusland L, Vialet-Chabrand S, Matthews J, Lawson T. 2015. Spatial and temporal responses in stomatal behaviour, photosynthesis and implications for water-use efficiency. In: Mancuso S, Shabala S, eds. *Rhythms in plants*. Heidelberg, Germany: Springer, 97–119.

Molnár-Láng M, Linc G, Szakács É. 2014. Wheat–barley hybridization: the last 40 years. *Euphytica* **195**: 315–329.

Morfopoulos C, Prentice IC, Keenan TF, Friedlingstein P, Medlyn BE, Peñuelas J, Possell M. 2013. A unifying conceptual model for the environmental responses of isoprene emissions from plants. *Annals of Botany* **112**: 1223–1238.

Mujeeb-Kazi A, Cortes A, Gul A, Farooq M, Majeed F, Ahmad I, Bux H, William M, Rosas V, Delgad R. 2008. Production and cytogenetics of a new *Thinopyrum elongatum*/*Triticum aestivum* hybrid, its amphiploid and backcross derivatives. *Pakistan Journal of Botany* **40**: 565–579.

Murchie EH, Kefauver S, Araus JL, Muller O, Rascher U, Flood PJ, Lawson T. 2018. Measuring the dynamic photosynthome. *Annals of Botany* **122**: 207–220.

Murchie E, Lawson T. 2013. Chlorophyll fluorescence analysis: a guide to good practice and understanding some new applications. *Journal of Experimental Botany* **64**: 3983–3998.

Murchie EH, Niyogi KK. 2011. Manipulation of photoprotection to improve plant photosynthesis. *Plant Physiology* **155**: 86–114.

Murchie E, Pinto M, Horton P. 2009. Agriculture and the new challenges for photosynthesis research. *New Phytologist* **181**: 532–552.

Murchie EH, Ruban AV. 2019. Dynamic non-photochemical quenching in plants: from molecular mechanism to productivity. *The Plant Journal* **101**: 885–896.

Orr DJ, Alcântara A, Kapralov MV, Andralojc PJ, Carmo-Silva E, Parry MAJ. 2016. Surveying Rubisco diversity and temperature response to improve crop photosynthetic efficiency. *Plant Physiology* **172**: 707–717.

Parry M, Andralojc P, Parmar S, Keys A, Habash D, Paul M, Alred R, Quick W, Servaites J. 1997. Regulation of Rubisco by inhibitors in the light. *Plant, Cell & Environment* **20**: 528–534.

Pearson M, Davies W, Mansfield T. 1995. Asymmetric responses of adaxial and abaxial stomata to elevated CO_2: impacts on the control of gas exchange by leaves. *Plant, Cell & Environment* **18**: 837–843.

Peleg Z, Fahima T, Abbo S, Krugman T, Nevo E, Yakir D, Saranga Y. 2005. Genetic diversity for drought resistance in wild emmer wheat and its ecogeographical associations. *Plant, Cell & Environment* **28**: 176–191.

Poorter H, Fiorani F, Pieruschka R, Wojciechowski T, van der Putten WH, Kleyer M, Schurr U, Postma J. 2016. Pampered inside, pestered outside? Differences and similarities between plants growing in controlled conditions and in the field. *New Phytologist* **212**: 838–855.

Prins A, Orr DJ, Andralojc PJ, Reynolds MP, Carmo-Silva E, Parry MA. 2016. Rubisco catalytic properties of wild and domesticated relatives provide scope for improving wheat photosynthesis. *Journal of Experimental Botany* **67**: 1827–1838.

Prohens J, Gramazio P, Plazas M, Dempewolf H, Kilian B, Díez MJ, Fita A, Herraiz FJ, Rodríguez-Burruezo A, Soler S *et al.* 2017. Introgressiomics: a new approach for using crop wild relatives in breeding for adaptation to climate change. *Euphytica* **213**: 158.

Quebbeman J, Ramirez J. 2016. Optimal allocation of leaf-level nitrogen: implications for covariation of V_{cmax} and J_{max} and photosynthetic downregulation. *Journal of Geophysical Research: Biogeosciences* **121**: 2464–2475.

R Core Team. 2016. *R: a language and environment for statistical computing. R v.3.6.1 (2019-07-05) – "Action of the Toes"*. Vienna, Austria: R Foundation for Statistical Computing. [WWW document] URL https://www.R-project.org/.

Rajaram S, Van Ginkel M, Fischer R. 1995. *CIMMYT's wheat breeding mega-environments (ME) Proceedings of the 8th international wheat genetic symposium, July 19–24, 1993*. Beijing, China: China Agricultural Scientech Press, 19–24.

Rasband WS. 1997–2018. ImageJ. US National Institutes of Health, Bethesda, MD, USA.

Ray DK, Mueller ND, West PC, Foley JA. 2013. Yield trends are insufficient to double global crop production by 2050. *PLoS ONE* **8**: e66428.

Reich PB, Walters MB, Ellsworth DS. 1997. From tropics to tundra: global convergence in plant functioning. *Proceedings of the National Academy of Sciences, USA* **94**: 13730–13734.

Reynolds M, Foulkes J, Furbank R, Griffiths S, King J, Murchie E, Parry M, Slafer G. 2012. Achieving yield gains in wheat. *Plant, Cell & Environment* **35**: 1799–1823.

Richards RA. 2000. Selectable traits to increase crop photosynthesis and yield of grain crops. *Journal of Experimental Botany* **51**: 447–458.

Rogers A, Medlyn BE, Dukes JS, Bonan G, Von Caemmerer S, Dietze MC, Kattge J, Leakey AD, Mercado LM, Niinemets Ü *et al.* 2017. A roadmap for improving the representation of photosynthesis in Earth system models. *New Phytologist* **213**: 22–42.

Salter WT, Merchant AM, Richards RA, Trethowan R, Buckley TN. 2019. Rate of photosynthetic induction in fluctuating light varies widely among genotypes of wheat. *Journal of Experimental Botany* **70**: 2787–2796.

Searles PS, Bloom AJ. 2003. Nitrate photo-assimilation in tomato leaves under short-term exposure to elevated carbon dioxide and low oxygen. *Plant, Cell & Environment* **26**: 1247–1255.

Sears E. 1955. An induced gene transfer from *Aegilops* to *Triticum*. *Genetics* **40**: 595.

Sears E. 1972. *Agropyron*–wheat transfers through induced homoeologous pairing. *Canadian Journal of Genetics and Cytology* **14**: 736.

Sebesta E, Wood E. 1978. Transfer of greenbug resistance from rye to wheat with X-rays. *Agronomy Abstracts* **70**: 61–62.

Silva-Perez V, Molero G, Serbin SP, Condon AG, Reynolds MP, Furbank RT, Evans JR. 2018. Hyperspectral reflectance as a tool to measure biochemical and physiological traits in wheat. *Journal of Experimental Botany* **69**: 483–496.

Tanaka Y, Adachi S, Yamori W. 2019. Natural genetic variation of the photosynthetic induction response to fluctuating light environment. *Current Opinion in Plant Biology* **49**: 52–59.

Taylor SH, Long SP. 2017. Slow induction of photosynthesis on shade to sun transitions in wheat may cost at least 21% of productivity. *Philosophical Transactions of the Royal Society B: Biological Sciences* **372**: e20160543.

Terashima I, Hanba YT, Tholen D, Niinmets U. 2010. Leaf functional anatomy in relation to photosynthesis. *Plant Physiology* **155**: 108–116.

Vialet-Chabrand S, Dreyer E, Brendel O. 2013. Performance of a new dynamic model for predicting diurnal time courses of stomatal conductance at the leaf level. *Plant, Cell & Environment* **36**: 1529–1546.

Vialet-Chabrand S, Lawson T. 2019. Dynamic leaf energy balance: deriving stomatal conductance from thermal imaging in a dynamic environment. *Journal of Experimental Botany* **70**: 2839–2855.

Vialet-Chabrand S, Lawson T. 2020. Thermography methods to assess stomatal behaviour in a dynamic environment. *Journal of Experimental Botany* **71**: 2329–2338.

Villareal R, Del Toro E, Rajaram S, Mujeeb-Kazi A. 1996. The effect of chromosome 1AL/1RS translocation on agronomic performance of 85 F_2-derived F_6 lines from three *Triticum aestivum* L. crosses. *Euphytica* **89**: 363–369.

Walker AP, Beckerman AP, Gu L, Kattge J, Cernusak LA, Domingues TF, Scales JC, Wohlfahrt G, Wullschleger SD, Woodward FI. 2014. The relationship of leaf photosynthetic traits – V_{cmax} and J_{max} – to leaf nitrogen, leaf phosphorus, and specific leaf area: a meta-analysis and modeling study. *Ecology and Evolution* **4**: 3218–3235.

Werner C, Ryel RJ, Correia O, Beyschlag W. 2001. Effects of photoinhibition on whole-plant carbon gain assessed with a photosynthesis model. *Plant, Cell & Environment* **24**: 27–40.

Whitney SM, von Caemmerer S, Hudson GS, Andrews TJ. 1999. Directed mutation of the Rubisco large subunit of tobacco influences photorespiration and growth. *Plant Physiology* **121**: 579–588.

Wong S, Cowan I, Farquhar G. 1979. Stomatal conductance correlates with photosynthetic capacity. *Nature* **282**: 424–426.

Wu A, Hammer GL, Doherty A, von Caemmerer S, Farquhar GD. 2019. Quantifying impacts of enhancing photosynthesis on crop yield. *Nature Plants* **5**: 380–388.

Yamori W, Nagai T, Makino A. 2011. The rate-limiting step for CO_2 assimilation at different temperatures is influenced by the leaf nitrogen content in several C_3 crop species. *Plant, Cell & Environment* **34**: 764–777.

Yamori W, Noguchi K, Terashima I. 2005. Temperature acclimation of photosynthesis in spinach leaves: analyses of photosynthetic components and temperature dependencies of photosynthetic partial reactions. *Plant, Cell & Environment* **28**: 536–547.

Zadoks JC, Chang TT, Konzak CF. 1974. A decimal code for the growth stages of cereals. *Weed Research* **14**: 415–421.

Zhu L, Bloomfield KJ, Hocart CH, Egerton JJ, O'Sullivan OS, Penillard A, Weerasinghe LK, Atkin OK. 2018. Plasticity of photosynthetic heat tolerance in plants adapted to thermally contrasting biomes. *Plant, Cell & Environment* **41**: 1251–1262.

Zhu X-G, Long SP, Ort DR. 2008. What is the maximum efficiency with which photosynthesis can convert solar energy into biomass? *Current Opinion in Biotechnology* **19**: 153–159.

Zhu X-G, Long SP, Ort DR. 2010. Improving photosynthetic efficiency for greater yield. *Annual Review of Plant Biology* **61**: 235–261.

Zhu XG, Ort DR, Whitmarsh J, Long SP. 2004. The slow reversibility of photosystem II thermal energy dissipation on transfer from high to low light may cause large losses in carbon gain by crop canopies: a theoretical analysis. *Journal of Experimental Botany* **55**: 1167–1175.

Zhu X-G, Song Q, Ort DR. 2012. Elements of a dynamic systems model of canopy photosynthesis. *Current Opinion in Plant Biology* **15**: 237–244.

Supporting Information

Additional Supporting Information may be found online in the Supporting Information section at the end of the article.

Fig. S1 Light saturated rates of CO_2 assimilation, carboxylation and electron transport in accessions from four wild relative genera and modern wheat cultivars.

Fig. S2 The internal CO_2 concentration (C_i) transition point, $C_{itransition}$ for 88 accessions across six genus groups.

Fig. S3 The maximum rate of *in vitro* carboxylation by Rubisco (V_{cmax}) determined for the modern *Triticum* varieties and four wild relative genera.

Fig. S4 Mean response of PSII operating efficiency (F_q'/F_m') to step changes in PPFD in *T. aestivum* and six genus groups.

Fig. S5 Steady-state non-photochemical quenching (NPQ) in five genus groups at1000 μmol m^{-2} s^{-1} PPFD.

Fig. S6 The relationship between A_{max} and specific leaf area (SLA) in five wild relative genera and modern wheat.

Fig. S7 Variation in specific leaf area (SLA) and percentage dry matter for five wild relative genera and modern wheat.

Fig. S8 Flag leaf absorbance of five genera in the wavelength region of 400–700 nm.

Fig. S9 Number of ears per plant for five wild relative genera and modern wheat.

Table S1 A summary of the wild relatives and traits successfully identified and/or introduced into modern wheat cultivar populations.

Table S2 Parameters from A vs C_i response curves including light- and CO_2 saturated photosynthetic rate (A_{max}), maximum carboxylation (V_{cmax}) and maximum electron transport (J_{max}) for 88 accessions across 5 genera.

Table S3 Significant comparisons between five genera for four chlorophyll fluorescence parameters measured under three PPFD intensities.

Please note: Wiley Blackwell are not responsible for the content or functionality of any Supporting Information supplied by the authors. Any queries (other than missing material) should be directed to the *New Phytologist* Central Office.